Journal of Tropical Pharmacy and Chemistry

Journal homepage: https://jtpc.jurnalfamul.com

Chemical, Spectral, Biological, and Toxicological Studies of Some Benzene Derivatives Used in Pharmaceuticals: In Silico Approach

Emranul Kabir[1, 2, 3,*], M R O Khan Noyon[1, 3], Md Rabiul Alam[4], Mr. Nasiruddin[5], Sajia Islam[1], Mahima Akter[6], Monir Uzzaman[1, 3,*]

[1]Faculty of Science, Department of Chemistry, University of Chittagong, Chittagong-4331, Bangladesh
[2]Department of Electrical and Electronic Engineering, International Islamic University Chittagong, Chittagong-4331, Bangladesh
[3]Department of Drug Design, Computer in Chemistry and Medicine Laboratory, Dhaka, Bangladesh
[4]Department of Chemistry, Comilla University, Koatbari, Cumilla-3506, Bangladesh
[5]Department of Chemistry, Bangabandhu Sheikh Mujibur Rahman Science and Technology University, Gopalganj, Bangladesh
[6]Department of Biochemistry and Molecular Biology, Jahangirnagar University, Dhaka, Bangladesh
*Corresponding author: ekabir05@gmail.com & monircu92@gmail.com

Abstract

The immune system of humans is impacted by many drugs. Chemicals that have a gender-bending impact on boys, were synthesized, their use spread, and as a consequence, they entered the ecology, the food chain, and eventually ended up in blood or human breast milk. Due to the use of benzene in both industry and medicine, chemicals with benzene rings are among the most problematic. The generation of benzene metabolites that produce superoxide, the phenoxy radical, and benzene-drug binding are only a few of the processes by which benzene and its derivatives cause harm. Benzene metabolites are distinct from chemical metabolites apart from benzene, which is lipophilic in nature and binds to cellular membranes, in that they bind to the intracellular plasma membrane where they produce degenerative alterations. Many diseases are associated with degenerative alterations in the mitochondria that culminate in mitochondrial dysfunction. Herein, twenty benzene derivatives (BDs) have been studied in terms of their biological and physiochemical properties, and the compounds have also been investigated using quantum mechanical computations. Binding affinities and behaviors of all BDs have been investigated using molecular docking and nonbonding interactions on 3D crystal structures of human receptor proteins serum albumin (1AO6), free native cellulase CEL48F (1G9G), and human D-amino acid oxidase mutant (P219L) complexed with benzoate (6KBP). Geometry as well as thermochemical data support the stability of all structures. All derivatives were predicted by ADMET to have improved pharmacokinetic properties and less acute oral toxicity.

Keywords: Benzene derivatives (BDs), Density functional theory, Thermochemistry, Molecular docking, and toxicology.

Received: 06 December 2023 **Accepted**: 28 November 2024

DOI: https://doi.org/10.25026/jtpc.v8i2.621

How to Cite:

Kabir, E., Noyon, M. R. O. K., Alam, M. R., Nasiruddin, M., Islam, S., Akter, M., Uzzaman, M., 2024. Chemical, Spectral, Biological, and Toxicological Studies of Some Benzene Derivatives Used in Pharmaceuticals; In Silico Approach. *J. Trop. Pharm. Chem.* **8**(2). 101-115. **DOI**: https://doi.org/10.25026/jtpc.v8i2.621

1 Introduction

In chemistry, the benzene ring is the most important fundamental structural component. In bioactive compounds and natural products, it is the most prevalent ring. Pharmaceuticals, plastics, oils, synthetic fibers and dyes all include benzene as a precursor [1]. Benzene-containing compounds can be found in over 500 medicines and agrochemicals [2]. Benzene derivatives (BDs) are organic compounds with a benzene moiety as the central component, giving them aromatic properties and increased structural stability [3]. The optimization and selection of the candidate for the supplementation of oral medicines, predicting human intestinal absorption (HIA) is a prime goal. The popularity of combinatorial chemistry techniques for drug design in which huge characters of novel compounds are synthesized and screened in parallel for in vitro pharmacological affectivity has sparked a surge in the desire for quick and accurate models for predicting HIA and other biopharmaceutical properties [4]. The novel percutaneous absorption results on benzene and derivatives are much acknowledged. The research is based on a human epidermis in vitro technique (diffusion cell method) [5]. BDs are commonly employed in numerous industrial applications. They are most typically utilized as solvents, oxidizers, additives, cooling mediators, and other polymers. The sorption of BDs on soils is preferred, and their removal is a tough process [6]. Chemicals that are produced by bacteria and other organisms could be at risk from food mesh in higher animals and humans. Due to their lipophilic nature, BDs in aquatic systems have the propensity to split into the organic layer and bioaccumulation inside the fatty tissues, resulting in greater concentrations [3, 7]. The pharmaceutical industry has a long history of therapeutic breakthroughs and innovative drug development due to the use of BDs [8]. The development of certain pharmaceutical medicines, such as antipsychotics, antidepressants, and aspirin (pain relievers) has been greatly aided by BDs [9]. Moreover, BDs have been essential in the development of other drug families, including antipsychotics, antidepressants, and antihistamines [10]. Concerns over toxicity and environmental impact have prompted research towards greener synthesis methods and safer alternatives, leading to ongoing innovations in medicinal chemistry [11, 12, 13]. The environment is constantly exposed to organic and inorganic chemicals, along with the mixtures of several chemical compounds; through their use in industrial approaches, chemical assays in research centers, and domestic utilization of different substances. The wastewater contains a wide range of BDs and combine actions of individual chemicals can lead to complicated and integrated toxic effects on the environment [14]. The entry of micropollutants into river flow or the loss of

insect biodiversity are two ecological effects related to the discharge of wastewater into fluvial environments [15, 16]. More attention has to be paid to the development of methods capable of evaluating the potentially dangerous effects of chemicals that affect living creatures. As a result, information on the environmental toxicity of commercial organic compounds especially the benzene derivatives are of importance [17]. The relationships of carcinogenic activity in aromatic compounds and their amino, alkyl-, nitro-analogs, and halo-alkanes support the concept of the enzymatic triggering of pro-carcinogens to proximate and ultimate carcinogens [18, 19]. The BDs are recognized to be the typical substrates for hydroxylation mediated by cytochrome P450. It is well known that the kind of substituent significantly influences the rate of oxidative stress on the yield of products that have been hydroxylated, as well as the cytotoxicity of substituted benzenes [19]. Consideration of the possibility of a novel candidate therapeutic molecule penetrating the blood-brain barrier (BBB) is a pivotal part of drug design [20]. In this perspective, Benzene and its derivatives are dealt with by chemists from various fields, including inorganic, polymer, physical, medicinal, and organic chemistry. For most of this whole century, scientists have examined the biological effects of benzene derivatives in human and animal models [21]. As seen by recent advancements, BDs have yielded promising new results in pharmaceutical companies. Treatments for many diseases, including cancer, neurological disorders, and infectious diseases, appear to be progressing due to technological advancements [22, 23]. The combination of computational modelling and high-throughput screening techniques has significantly expedited the identification of lead compounds, thereby enhancing the drug discovery process. Furthermore, advancements in computational methodologies have enabled the efficiency of BDs, addressing previous concerns regarding their environmental impact and sustainability. Overall, these recent achievements underscore the continued importance of BDs in shaping the future of pharmaceuticals and improving global healthcare.

In this study, we optimized benzene and its twenty analogs' using quantum computation to examine their biological behavior. We estimated the change of free energy, enthalpy, dipole-moment, electrostatic potential, HOMO–LUMO energy gap, hardness, and softness. The binding score, mode(s), and interactions of ligands with amino acid sequences of the receptor protein have been analyzed by molecular modeling as well as non-bonding interactions. The majority of the derivatives demonstrated increased thermal steadiness, chemical reactivity, binding aptitudes, and interactions. Hydrogen bonding is important in biological processes as it affects the system's thermodynamic and structural stability [24, 25].

2 Materials and Methods

2.1 Geometry optimization

All BDs original geometries were obtained from PubChem, an online resource of chemical structures. The application Gaussian 09W Revision D.01 was used for modification and geometry optimization [26]. To determine the lowest energy conformer, a molecular dynamic, and conformational study was carried out using an Amber force field using Gabedit software (2.5.0) at ambient temperature (298.15 K) and pressure (1.00 atm) [27]. The conformers of lowest energy were optimized by using density functional theory (DFT) [28] along with the B3LYP [29] 6-31g (d, p) [30] basis set. Molecular orbital characteristics were calculated by last reported methods [31]. Employing time-dependent density functional theory (TD-DFT), the electronic transition was computed [32].

2.2 Protein preparation, and visualization

The 3D crystalline structure of the receptor protein was retrieved from the RCSB data bank of proteins using PDB IDs 1AO6, 1G9G and 6KBP which have equivalent resolutions of 2.50 Å, 1.90 Å, and 2.25 Å respectively. Water molecules, heteroatom, and co-crystallized ligands were eliminated by Discovery Studio 2021 software. The energy was minimized by employing the Swiss PDB viewer program (version 4.1.0). Finally, PyRX software (ver. 0.8) was utilized to perform molecular docking identifying the protein as a macromolecule and the compound as a ligand. Individual grid box was maintained for three receptor proteins with X, Y, and Z dimensions of 74.04 Å, 60.62 Å, and

74.60 Å for **1A06**; 65.36 Å, 64.09 Å, and 62.15 Å for **1G9G**, and 42.56 Å, 65.31 Å, and 62.74 Å for **6KBP** respectively. Further, docked compounds and prepared protein were saved together to prepare the complex for interaction calculation.

2.3 Pharmacokinetic prediction

Pharmacokinetic (PK) inspection of drugs is designed in preclinical functional species (usually mice) to confirm that a proposed medicine has the requisite exposure to ensure efficiency following in-vitro dosing [33]. The term pharmacodynamics (PD) refers to how medicine impacts the body. At present, any software can anticipate both PK and PD. For cost minimization as well as time consumption, "Adsorption, distribution, metabolism, excretion, and toxicity (ADMET)" data helps to develop a method to design a new drug before its synthesis. In the present investigation, ADMET of **20** benzene derivatives was predicted using the *admetSAR* protocol [34] and presented in **Figure 1**. In all cases, "SMILES (simplified molecular input line entry system)" and structural data files were used during the generation process.

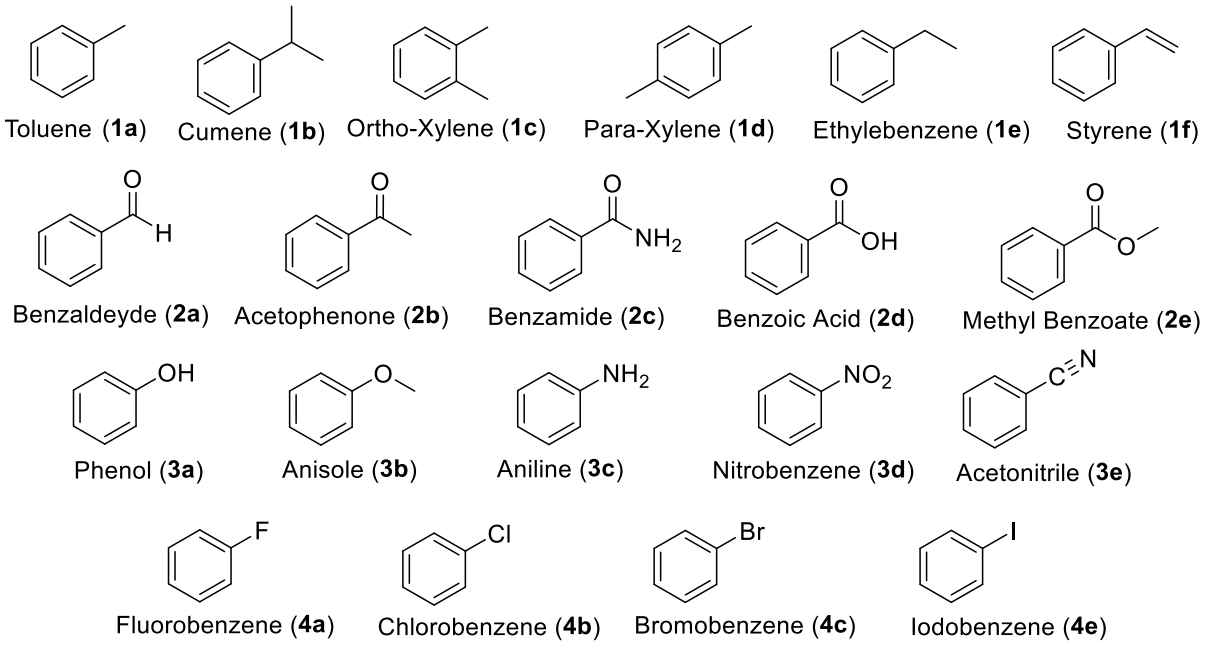

Figure 1 Chemical structures of studied benzene derivatives.

3 Results and Discussion

3.1 Equilibrium geometry

Due to the existence of different functional groups in the structure of different BDs, it is crucial to calculate the bond lengths as well as bond angles to know the equilibrium geometry in detail [35]. Equilibrium geometry is a key element in any chemical species' structural characterization because it gives minimum strain to a molecule. Lists of certain bond lengths and angles for benzene and its derivatives are shown in **Tables S1** and **S2** (for atom numbers see the optimized structures in **Figure S1**). The bond lengths of the derivatives have not changed much from the experimental values, but the occupancy of different functional groups enhances the possibility of changing the bond length of molecules present around it. In our studied analog, we have arranged the BDs in four different series for better analysis purposes according to the presence of electron donor and receiver at the functional groups. Here, the bond length between the carbon of the benzene ring and the central atom of functional group is the decider of the chemical reactivity. In **1(a-e)** the presence of electron density lowers the bond length; we can see that the lowest bond length was found in the C1-C7 bond in analog **1f** and

the highest was found in the C1-C2 bond in **1b.** In series **2(a-e)**, the bond length of the compounds changes due to the existence of electron-donating groups attached to the carbonyl group in the side chain. With the inclusion of powerful electron-donating groups, the bond length increases. In compound **2(c)**, the NH_2 group increases the electron density at the core of the carbonyl group which results in the highest bond length in the C3-C9 bond in this series and there is no electron donor group in **2a**, which is the reason for the lowest bond length in the C2-C8 bond. The presence of the electron-withdrawing group in series **3(a-e)** increases the bond length. The NO_2 group linked to the benzene ring is the reason for the highest bond length of analog **3d** in the series and the lowest had been observed in **3b**. In the case of halo benzene, the bond length enlarges with the increase in the size of the halogen atom. Hence, we found that fluorobenzene (**4a**) has the lowest bond length and iodobenzene (**4d**) has the highest bond length. There were some changes in the case of bond angles. Slightly increased bond angles were observed in C1-C2-C5 of **1a**, C2-C3-C6 of **1e**, C1-C7-C8 of **1f**, and slightly lower bond angles in H10-C1-C3 of **1b**.

3.2 Thermodynamic analysis

Thermochemical computations enable the prediction of reaction kinetics and chemical stability of the compounds. The extent of the spontaneity of an adsorption system is reflected by the free energy value, and the negative sign denotes the reaction's spontaneity condition. The impetuosity of a reaction and stability of a product can be evaluated from its free energy, enthalpy, and electronic energy [36]. Here **16** compounds out of **20** BDs, exhibited negative results for free energy and enthalpy **(Table 1** and **S3)** except **4(a-d),** implying that no external energy will be required for binding. Compounds **4(a-d)** showed less binding interaction than other derivatives due to the less steric effect and chemical interaction with a single halogen group (X = F, Cl, Br, I). Higher internal (ΔE) and free energy (ΔG) values, as well as high negative enthalpy (ΔH) value (-459.987 Hartree), imply that **2e** containing its $COOCH_3$ functional group has superior thermodynamic properties than other benzene analogs. Here, enthalpy values of **2a** and **1a** are -345.465 Hartree and -271.444 Hartree respectively containing CHO and CH_3 functional groups in their chemical structures. The electrical property of a molecule is depicted by its dipole moment value, with a high dipole moment value resulting in more intermolecular interactions. A more polar nature is indicated by a high dipole moment value [37, 38]. From **Table 1** and **S3**, **3d** (4.557 Debye) had the best dipole moment, indicating a strong binding score, hydrogen bonding, and non-binding actions in the drug-receptor complex while **1a** showed a lower dipole moment with less binding interaction. In our investigation, compounds **2(a-c)** showed significant dipole moment values of 3.498 Debye, 3.283 Debye, and 2.983 Debye respectively. Again, the analogs **3d** and **3e** exhibited substantial dipole moments 4.557 Debye and 4.546 Debye respectively for the existence of comparatively better electron-withdrawing functional groups with negative inductive effects. In the case of the halo-benzene analogs, **4b** (1.920 Debye) exhibited a comparatively high dipole moment.

Table 1 Molecular formula (MF), molecular weight (MW), energies (Hartree), and dipole moment (Debye) of benzene and its studied analogs. (Remaining data are included in Table S3)

Name	MF	MW	Internal Energy	Enthalpy	Gibbs Free Energy	Dipole Moment
Benzene	C_6H_6	78.110	-232.153	-232.152	-232.183	0.000
1(a).	C_7H_8	92.140	-271.445	-271.444	-271.482	0.342
1(b).	C_9H_{12}	120.190	-350.017	-350.016	-350.059	0.284
1(d).	C_8H_{10}	106.160	-310.735	-310.734	-310.774	0.585
1(f).	C_8H_8	104.150	-309.521	-309.519	-309.559	0.187
2(a).	C_7H_6O	106.124	-345.466	-345.465	-345.503	3.283
2(e).	$C_8H_8O_2$	136.150	-459.988	-459.987	-460.031	1.851
3(c).	$C_6H_5NH_2$	93.130	-287.493	-287.493	-287.528	1.709
3(d).	$C_6H_5NO_2$	123.110	-436.648	-436.647	-436.687	4.557
4(a).	C_6H_5F	96.104	61.241	61.833	39.930	1.349
4(c).	C_6H_5Br	157.010	60.483	61.075	37.539	1.812

Table 2 Energy (eV) of HOMO-LUMO, gap, hardness (η), softness (S), chemical potential (μ), electronegativity (χ), and electrophilicity (ω) of benzene and some of its studied derivatives. (Remaining data are included in Table S4)

Name	εHOMO	εLUMO	Gap	η	S	μ	χ	ω
Benzene	-6.721	0.082	6.803	3.402	0.147	-3.320	3.320	1.620
1(a).	-6.412	0.122	6.534	3.267	0.306	-3.145	3.145	1.514
1(b).	-6.422	0.098	6.520	3.260	0.153	-3.162	3.162	1.533
1(d).	-6.150	0.163	6.313	3.157	0.158	-2.994	2.994	1.420
1(f).	-6.046	-0.853	5.193	2.597	0.385	-3.449	3.449	2.291
2(a).	-6.966	-1.796	5.170	2.585	0.386	-4.381	2.191	4.514
2(e).	-7.129	-1.790	5.339	2.670	0.375	-4.460	2.230	3.725
3(c).	-5.393	0.233	5.626	2.813	0.355	-2.580	2.580	1.183
3(d).	-7.602	-2.435	5.167	2.584	0.387	-5.019	5.019	4.874
4(a).	-5.552	-0.603	4.949	2.474	0.202	-3.077	3.077	11.716
4(c).	-6.714	-0.365	6.348	3.174	0.158	-3.539	3.539	19.882

3.3 Frontier Molecular orbital analysis

The result of frontier molecular orbital plays an evidential role in the attainment of the potential energy required for chemical reactions. For many chemical reactions, the HOMO (Highest Occupied Molecular Orbital) and LUMO (Lowest Unoccupied Molecular Orbital) play a vital role [39]. The transition from HOMO to LUMO is affiliated with electronic absorption [40]. Both chemical hardness and softness are influenced by the HOMO-LUMO gap value. A molecule's prolonged energy gap is linked to both high chemical stability and low chemical reactivity. Due to the ease of electron transition, a minimal gap of energy is related to equally weak chemical stability and strong chemical reactivity [41]. From **Table 2, S4** and **Figure S2,** it is evident that benzene has the highest energy gap value, chemical hardness, and lowest softness of all the derivatives. But among all BDs, compound **1e** has the highest energy gap value (6.544 eV) and **4a** has the lowest energy gap value (4.949 eV) compared to the other benzene derivatives. The analog **1e** has chemical stiffness and pliability values of 3.272 eV and 0.306 eV respectively, where the chemical hardness value is at the peak of all the derivatives. In contrast, **4a** has a chemical hardness of 2.474 eV and a softness of 0.202 eV, where the chemical hardness value is the lowest among all the BDs. The lowest softness value among the derivatives is 0.153 eV, which is of the analog **1b**. Further, **4a** has a stronger electron-withdrawing group fluorine (F) group connected to the benzene ring which is a reason behind the higher chemical reactivity.

3.4 Electrostatic potential analysis

The total charge density of the electrons and nuclei is shown by the molecular electrostatic potential (MEP) map and reveals information on the electro-negativity, partial charge, dipole moment, and chemical reactivity of the molecule [42]. The analysis of the biological recognition mechanism and hydrogen bonding interaction can also be interpreted by it [43]. By using the colors blue and red, it depicts a potential electrophilic and nucleophilic attack [44]. Green represents zero potential areas, blue indicates the highest positive area which is more favorable for the nucleophilic attack, and the greatest negative area, which is red, is conducive to electrophilic attack. From the MEP map (**Figure S3**) it can be seen that the areas with negative potentialities are over electronegative atoms (e.g., O, Cl, F, Br, etc.), and those having positive potential are over hydrogen atoms. Here, benzene derivatives **1(a-f)** showed the range of negative and positive potentiality '-2.384e-2 - 2.825e-2' in which **1(a-e)** exhibited higher electrostatic potentiality than that of benzene due to the presence of various alkyl groups in different position whereas **2(a-e)** and **3(a-e)** showed the range of negative and positive potentiality '-5.081e-2 - 5.879e-2' and '-3.190e-2 – 6.255e-2' respectively in which all of the derivatives exhibited higher electrostatic potentiality than that of benzene due to the occupancy of high electronegative O and N atoms in the functional groups of their structures. Again, the BDs **4(a-d)** showed the range of negative and positive potentiality '-2.084e-2 - 3.827e1' in which only **4d** exhibited higher electrostatic potentiality than that of benzene (**Table S5**).

3.5 Vibrational frequency analysis

The vibrations of molecules are examined via infrared spectroscopy. Functional groups can be related to distinctive infrared absorption bands which correspond to their fundamental vibrations [45]. FT-IR spectral data for BDs are presented in **Table S6**. For all compounds, the FT-IR spectral frequencies are found to be in the range of 400–4000 cm^{-1} (**Figure 2a** and **Table S6)**. For the precision in their concordance with the experimental data, the estimated FT-IR vibration wave numbers of the benzene analogs have been multiplied by the magnification factor of 0.9679, and their provisional vibrational assignments have been reported [37]. The aromatic benzene and its analogs displayed symmetrical vibration stretching for the C-H bond in the region 3175-3185 cm^{-1}, but asymmetric vibration frequencies have been seen in the considerably lower range [46]. The distinctive C=O stretching vibration is seen in the BDs **2(a-e)** between 1775 and 1800 cm^{-1}. The C-H stretching vibration at the range 3168-3170 cm^{-1} in **2b** proves the presence of an aliphatic methyl group (CH_3) [47]. The hydroxyl (OH) functional group shows the stretching vibration in the range 3766-3770 cm^{-1} and verifies the presence of carboxylic OH in **2d** [48]. Again, both the C-H and C-O stretching vibration at the range 3172-3175 cm^{-1} and 1001-1005 cm^{-1} respectively confirms the existence of aliphatic methyl group (CH_3) and carboxylic ester (COO) group in the **2e** [49]. The analog **3a** shows the O-H stretching vibration at the range 3820-3825 cm^{-1}, whereas the existence of methoxy group (OCH_3) in **3b** is confirmed by the distinctive O-CH_3 and C-H stretching vibrations which are shown in the regions of 1075-1080 cm^{-1} and 3145-3150 cm^{-1}, respectively [50]. The analog **3c** exhibits N-H stretching vibration between 3565 and 3570 cm^{-1}. Again, the existence of cyano functionality (CN) in **3e** is confirmed by the stretching vibration in the range of 2345-2350 cm^{-1} [51], which is greater than the C-N symmetric stretching in the range of 1395–1400 cm^{-1} for **3d**. In benzene analogs **4(a–e)**, remarkably lower vibration frequency bands at 855–865 cm^{-1} identify the existence of a carbon-halogen bond [52].

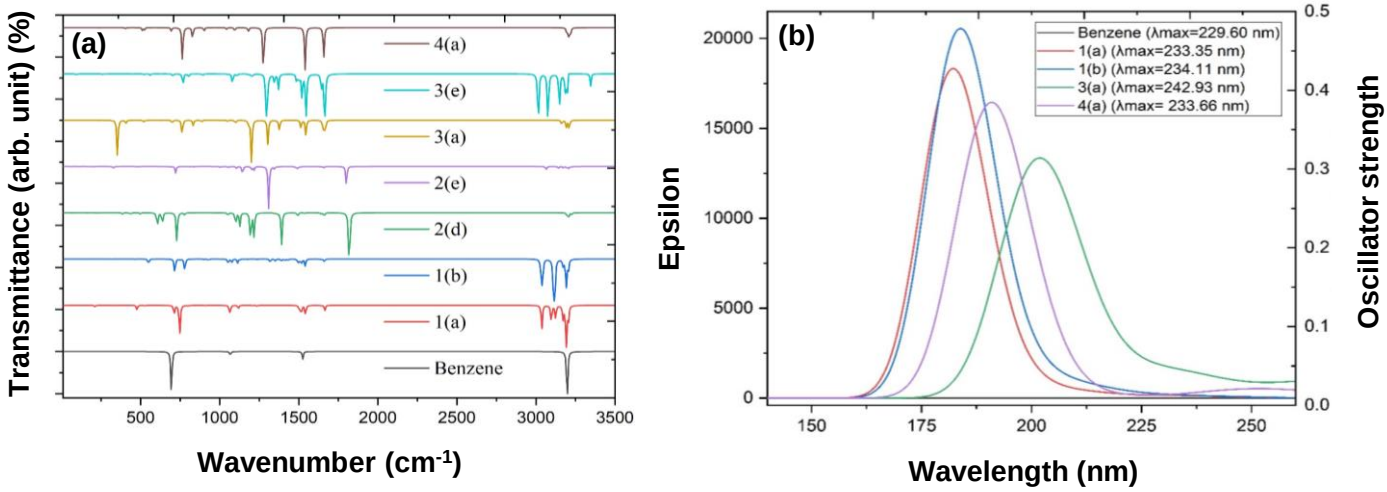

Figure 2 (a) FT-IR and (b) UV-Vis spectra of benzene and some of its selected derivatives.

3.6 UV-Vis spectral analysis

A standard for the study of molecular orbital of aromatic ring systems using time-dependent density functional theory (TD-DFT) is UV-visible spectroscopy, which ensures a balance between accuracy and computing expense. **Table S7** and **Figure 2b** show each of the two distinctive electronic transition states from the analogs. Kinetic stability and chemical reactivity in this investigation are determined by the initial transition of electrons from the

ground state (S_0) to singlet (S_1) [38]. Analogs **2a**, **2d** and **3(d-e)** showed a broad absorption band at wavelengths of 351.52 nm, 285.50 nm, 409.39 nm, and 241.03 nm, along with their oscillator strengths of 0.000, 0.000, 0.000, and 0.009, respectively. Charge transfer of the electrons to the excited state S_0 to S_1 results in maximum wavelength of the configurations; [0.694(H→L), -0.133(H → L+3)] for **2a**, [0.693 (H-2→L), 0.132 (H-2→L+2)] for **2d**, [0.698(H→L), -0.108(H→L+2)] for **3d** and [0.535 (H-1→L), -0.125 (H-1→ L+1), -0.205(H→L), -0.393 (H→L+1)] for **3e**. The electronic movement from HOMO to LUMO is the major root of the two broad absorption band wavelengths with the highest intensities, which are 351.52 nm, 285.50 nm, 409.39 nm, and 241.03 nm, respectively. The presence of electron-withdrawing CHO, COOH, $–NO_2$, and CN groups in the analogs **2a, 2d, 3d** and **3e** respectively make the compound more reactive towards addition reaction by decreasing the electron density in the benzene ring. The higher excitation energy corresponding to the HOMO–LUMO energy gaps increases the kinetic stability and decreases the chemical reactivity as it is energetically unfavorable and lower excitation energy minimizes the kinetic stability and maximizes the chemical reactivity [41]. Thus, analogs **2a, 2d, 3d** and **3e** have more reaction sites, which are ensured by the lower excitation energies; 3.527 eV, 4.343 eV, 3.029 eV, and 5.144 eV, respectively. On the other hand, **1a** has the least reaction sites as it possesses the highest excitation energy and oscillator strength of 0.003 for the transition S_0 to S_1. The electron donor CH_3 group connected to the benzene ring makes the compound less reactive in the addition reaction. The other analogs; **1(b-e), 2(b-c), 2e, 3(a-c),** and **4(b-d)** have moderate reactive sites with excitation energies at a range of 3.545 eV to 5.217 eV.

3.7 Molecular docking and non-bonding interactions analysis

Molecular docking is a technique that is used to forecast the preferred orientation, affinity, and interaction of a lite molecule ligand and a protein at the atomic level, which permits to investigate of the behavior of the ligand in the binding site of the target protein and to elucidate the fundamental biochemical processes [53]. In **Table S8**, average binding scores and ligand-protein interactions are summarized. Here, the higher negative binding values represent the stronger bonds between the receptor protein and benzene derivatives. Multiple non-covalent interactions like hydrogen bonds, halogen bonds as well as hydrophobic interactions are related to the binding of examined structures. However, from theory, it is stated that hydrogen bonds less than 2.3 Å are considered strong enough to increase the binding affinity by some magnitude [54]. In halogen analogs, **4(a-d)–1G9G** docked conformers (**Figure 3**), the binding affinity values are similar (≈ -5.5 Kcal/mol) and relatively low, as there is no hydrogen bond formed between halogen and 1G9G instead formed π-alkyl bonding with ALA228 at a distance of 5.08567 Å and over and π-π stacked bonding with the residue TRP154. This indicates they bind weakly with the receptor protein. Analogs **2(a-b)** and **2(d-e)** were docked with receptor protein 6KBP (**Figure S4**). Among these, analog **2e** shows the highest binding affinity value of -6.4 Kcal/mol and contains one hydrogen bond with TYR228 at a distance of 2.44943 and two hydrogen bonds with ARG283 at a distance of 2.01817 and 2.20044 Å, and an effective carbon-hydrogen bond with GLY313 at 2.74732 Å distance. The low binding affinity value of **2a** (-5.8 Kcal/mol) is due to the larger bond distance (over 2.47 Å) than the experimental limit (2.30 Å) in one of the hydrogen bonds. Receptor protein 1AO6 is docked with **2c** and **3(a-e)** (**Figure 3**). The analog **3d** has one hydrogen bond with ARG410 at a distance of 2.35701 Å and hence shows a higher binding affinity of -6.0 Kcal/mol. However, analogs **3a** and **3c** have the same binding affinity of -5.0 Kcal/mol as they may interact through π-alkyl bonds with LEU407, LEU430, and LEU453. Most of the benzene derivatives bind with either TYR228 or ARG283 within the active site of receptor protein through hydrogen bonding, which might indicate that hydrogen bonding with these amino acids is stronger and shows higher binding affinity values. However, analog **3b** exhibits the lowest binding affinity value -4.9 Kcal/mol as it forms hydrogen bonds with ARG257 and ARG257. One of the most common interactions is π-alkyl, and this interaction is found in almost all derivatives with the LEU238,

ALA291, LEU430, LEU453, LEU407, LEU260, VAL433, PHE180, TYR403, TRP154, residues respectively. Another two significant residues are π-π stacked as well as π-π T-shaped with the residue TYR230, TYR224, TRP154, and TYR231, TYR228, and TRP298, respectively.

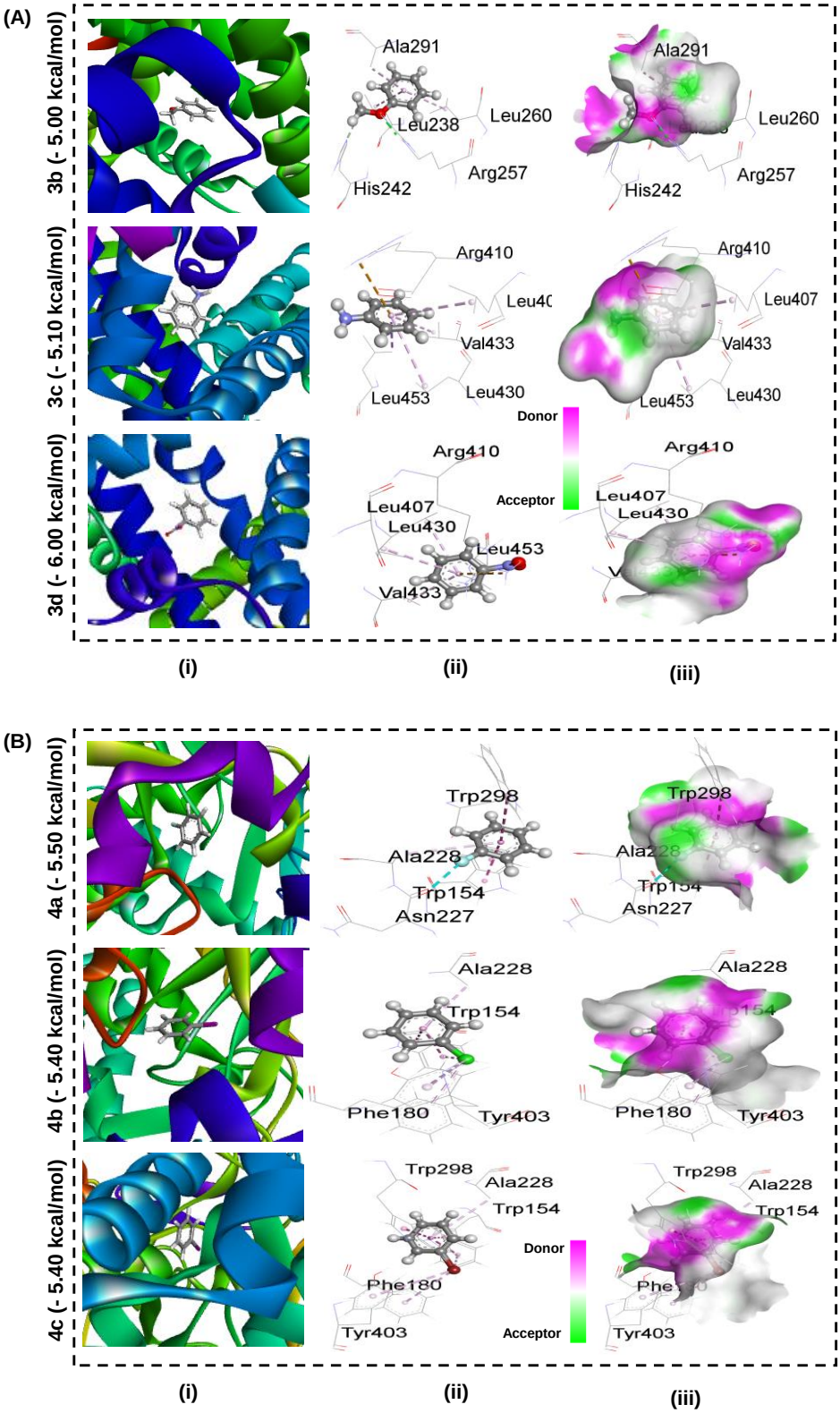

Figure 3 (i) Docked conformer, **(ii)** Non-bonding interactions and (iii) hydrogen bond surface for **(A)** 3b, 3c and 3d compounds with protein 1AO6 and **(B)** 4a,4b and 4c compounds with protein 1G9G respectively.

3.8 ADMET analysis

The body's response to a drug, which is investigated in pharmacokinetics, is referred to as "Adsorption, distribution, metabolism, excretion, and toxicity (ADMET)" [55]. As a result, it is necessary for drug design, and also ADMET testing, which is used to assess all the possible drug aspects [37]. The *admetSAR* online database represents the *admet* properties of various BDs. In the tabulated (**Table S9)** *admetSAR* data human intestinal absorption (HIA), human oral bioavailability (HOB), *p*-glycoprotein inhibitor (*p*-Gp-I), blood-brain barrier (BBB), cyp-glycoprotein inhibitor (CYP3A4-I), human ether-a-go-go, go-related gene (hERG), carcinogenicity, acute oral toxicity (AOT), rat acute toxicity (RAT) and biodegradation properties are in the list. However, *admetSAR* data showed that all benzene derivatives have a positive response to HIA in the range of +1.000 to +0.601, which suggests that all compounds cannot be excreted more readily by urinary and rectal routes [56]. In our investigation, all BDs showed higher HIA values than benzene (+0.992) except the analogs **1c**, **4c** and **4d**. Almost all of the compounds exhibited the same positive results for HOB except compound **2d** (+0.85). Positive human oral bioavailability has the possibility of causing health problems [34]. The BDs **2a**, **2b** and **3a** exhibited greater C2P values than benzene (+0.909). The BBB is a highly restrictive barrier that tightly regulates the movement of molecules, ions, and cells between the body's nervous system and the brain. The nervous system (CNS) is shielded by this barrier from toxins, infections, inflammation, damage, and illness [57]. In our investigation, all of the benzene derivatives exhibited a positive response to BBB in the limit of +0.996 to +0.908 which is alarming. Positive responses reveal that these will not go through BBB very quickly [58]. Here, the parent compound benzene showed better BBB (+1.000) which is comparatively greater than all BDs. All of the benzene analogs have non-inhibition of *p*-glycoprotein, which suggests that no one has any effect on *p*-glucosylphosphorus [59]. According to its roles, the *p*-Gp-I or *p*-Gp-S mostly acts as an activator or regulator, when it is triggered [60].

These benzene analogs do not affect CYP3A4 inhibition or substrate binding. All of the investigated compounds have weakly affected (+0.957 to +0.804) the human ether-a-go-go related gene (hERG), which can cause long QT syndrome, cardiac adverse effects, and mortality [61]. Carcinogens are compounds or chemicals that mix, in some circumstances, and after prolonged or severe exposure, have the potential to cause cancer in humans [62]. In this study, BDs **1b, 1d** and **3d** exhibited carcinogenic toxicity whereas the remaining benzene analogs were non-carcinogenic like benzene. All BDs and also benzene showed acute oral toxicity level III, meaning they are comparatively less dangerous, except for **3a, 3c** and **3d** which display acute oral toxicity in level II [63]. Here all of the investigated analogs predicted LD_{50} values comparatively safe in the range of 1.447-2.539 mol/Kg [64]. The biodegradation of substances is one of the most vital factors that influence toxicity and the ultimate destiny of an organic chemical in aquatic and terrestrial ecosystems is the method through which organic compounds are released into the environment [65]. In our investigation, benzene and most of its analogs were readily biodegradable except the compounds **3d** and **4(a-d)** which showed non-biodegradable activity.

3.9 PASS prediction analysis

The "prediction of activity spectra for substances (PASS)" is a digital tool that has been used to foretell the outcomes of over a thousand biological and toxicological studies [66]. The probability of a molecule being active or inactive ranges from 0.000 to 1.000. Here, the predicted results are expressed using only the P_a (probability of compound becoming active) values presented in **Table S10**. Here, **Table S10** depicts the analysis of predicted results. According to PASS predictions, none of the chemicals has the active potential to show biological function. Analgesics are drugs that, without affecting cognition, selectively reduce pain by acting on peripheral and central nervous system (CNS) pain mediators. Both central and peripheral pain models are included to make the test for the analgesic property more obvious. In our analysis, both **4a** and **4b**

exhibited better analgesic properties than benzene, where 4a showed the most activity (Pa = 0.593) among all BDs. Non-steroidal anti-inflammatory drugs typically exhibit antipyretic activity as one of their features as a result of their inhibition of prostaglandin formation in the central nervous system. A prostaglandin-induced rise in body temperature is suppressed by antipyretics. Here, compound **2d** represents the most probable antipyretic activity (P_a= 0.593). In **Table S10** the BDs **1b, 1d 2(b-e)** and **3(a, b)** exhibited better antipyretic efficacy than the benzene. A drug or treatment that lessens inflammation or swelling is said to have anti-inflammatory properties [67]. In this analysis, both compounds **1b** and **3e** exhibited comparatively good anti-inflammatory activities (P_a) which are 0.650 and 0.662 respectively. Here, almost all of the BDs showed better anti-inflammation activity than the benzene except **4c**. The formation of the cell components in both blood and plasma is known as hematopoiesis. The hematopoietic system comprises organs and tissues like the bone marrow, liver, and spleen. In our investigation, compound **3c** showed the highest hematopoietic inhibitory effect (P_a = 0.611) which is also greater than benzene (P_a = 0.608). In **Table S10**, none of the compounds exhibited any promising biological effect in the case of both gastrointestinal motility stimulants and diabetic nephropathy treatment. Viral infections can be treated with a class of medications referred to as antiviral drugs [68]. In our study, many of the benzene analogs showed promising antiviral activity (P_a) against, picornavirus, rhinovirus influenza, and hepatitis B. The analog **3d** showed the most promising antiviral activity (P_a = 0.714) against picornavirus which is also better than benzene (P_a = 0.676). The similarity of a drug substance is measured by using Lipinski's rule of five to assess if it is orally active as a medicinal molecule [69]. In our research, practically the entire tested compound had similar oral bioavailability scores due to their activity of functional groups.

4 Conclusions

Benzene and its derivatives are the key components of the modern pharmaceutical industry. These are mostly utilized as an intermediate to synthesize other chemicals. Our study looked at a computational analysis of twenty different benzene derivatives. All structures were supported by analyses of optimum geometries, vibration frequencies, and UV-visible spectral data. All investigated benzene derivatives exhibited thermal stability, significant binding affinity, and nonbonding interaction with three receptor proteins (1A06, 1G9G, and 6KBP). Most of the benzene derivatives bind with the active site of receptor protein through hydrogen bonding, which might indicate that hydrogen bonding with these amino acids is stronger and shows higher binding affinity values. All tested benzene analogs may have improved oral absorption abilities because all of them predicted LD_{50} values comparatively safe in the range and acute toxicity in category III with higher pharmacokinetic properties. Due to concern and increasingly restrictive legislation, our inquiry is presenting the results of biological and ecological studies on a few benzene derivatives utilized in pharmaceuticals.

5 Declarations

5.1 Acknowledgment

The authors are thankful to the Department of Drug Design, Computer in Chemistry and Medicine Laboratory, Dhaka, Bangladesh for their continuous support and suggestions.

5.2 Authors' contribution

In this work, each author made an equal contribution.

5.3 Funding

This research did not receive any external economic support.

5.4 Conflict of interest

The authors declare no conflict of interest.

6 Supplementary Data

Supporting information article can be accessed online.

7 References

[1] Mykhailiuk, P. K. Saturated Bioisosteres of Benzene: Where to Go Next? *Org Biomol Chem*, **2019**, *17* (11), 2839–2849. https://doi.org/10.1039/c8ob02812e.

[2] Denisenko, A.; Garbuz, P.; Shishkina, S. V.; Voloshchuk, N. M.; Mykhailiuk, P. K. Saturated Bioisosteres of Ortho -Substituted Benzenes. *Angewandte Chemie*, **2020**, *132* (46), 20696–20702. https://doi.org/10.1002/ange.202004183.

[3] Gupta, S.; Basant, N.; Singh, K. P. Predicting Aquatic Toxicities of Benzene Derivatives in Multiple Test Species Using Local, Global and Interspecies QSTR Modeling Approaches. *RSC Adv*, **2015**, *5* (87), 71153–71163. https://doi.org/10.1039/c5ra12825k.

[4] Wessel, M. D.; Jurs, P. C.; Tolan, J. W.; Muskal, S. M. Prediction of Human Intestinal Absorption of Drug Compounds from Molecular Structure. *J Chem Inf Comput Sci*, **1998**, *38* (4), 726–735. https://doi.org/10.1021/ci980029a.

[5] Nies, E.; Korinth, G. Commentary on "Penetration of Benzene, Toluene, and Xylenes Contained in Gasolines through Human Abdominal Skin in Vitro." *Toxicology in Vitro*, **2008**, *22* (1), 275–277. https://doi.org/10.1016/j.tiv.2007.04.015.

[6] Ghasemi, J. B.; Salahinejad, M.; Rofouei, M. K.; Mousazadeh, M. H. Docking and 3D-QSAR Study of Stability Constants of Benzene Derivatives as Environmental Pollutants with α-Cyclodextrin. *J Incl Phenom Macrocycl Chem*, **2012**, *73* (1–4), 405–413. https://doi.org/10.1007/s10847-011-0078-4.

[7] Journal, I.; Science, P.; Available, H. C. Genotoxicity of Benzene and Soluble Benzene Substituted Organic Compounds in Mammals- A Review. **2014**, *4* (4), 24–39.

[8] Ang, D.; Kendall, R.; Atamian, H. Virtual and In Vitro Screening of Natural Products Identifies Indole and Benzene Derivatives as Inhibitors of SARS-CoV-2 Main Protease (Mpro). *Biology (Basel)*, **2023**, *12* (4), 519. https://doi.org/10.3390/biology12040519.

[9] Patil, S. B. Biological and Pharmacological Significance of Benzimidazole Derivatives: A Review MEDICINAL SIGNIFICANCE OF BENZIMIDAZOLE ANALOGUES: A REVIEW. *Article in International Journal of Pharmaceutical Sciences and Research*, **2020**, *11* (6), 2649–2654. https://doi.org/10.13040/IJPSR.0975-8232.11(6).2649-54.

[10] Volz, H.-P.; Laux, G. Tricyclics: Imipramine, Clomipramine, Trimipramine (Dibenzazepines). In *NeuroPsychopharmacotherapy*; Springer International Publishing: Cham, **2022**, 1–11. https://doi.org/10.1007/978-3-319-56015-1_385-1.

[11] Nambela, L.; Haule, L. V.; Mgani, Q. A Review on Source, Chemistry, Green Synthesis and Application of Textile Colorants. *J Clean Prod*, **2020**, *246*, 119036. https://doi.org/10.1016/J.JCLEPRO.2019.119036.

[12] Vessally, E.; Mohammadi, S.; Abdoli, M.; Hosseinian, A. *Convenient and Robust Metal-Free Synthesis of Benzazole-2-Ones Through the Reaction of Aniline Derivatives and Sodium Cyanate in Aqueous Medium*; **2020**, *39(5),* 11-19.

[13] Nardi, M.; Cano, N. C. H.; Simeonov, S.; Bence, R.; Kurutos, A.; Scarpelli, R.; Wunderlin, D.; Procopio, A. A Review on the Green Synthesis of Benzimidazole Derivatives and Their Pharmacological Activities. *Catalysts*, **2023**, *13* (2), 392. https://doi.org/10.3390/catal13020392.

[14] Castillo-Garit, J. A.; González Pérez, Y.; Albear, E. M.; Rodríguez, E.; Pérez-Doñate, V.; Pérez-Giménez, F. Environmental Toxicity Prediction Using Computational Tools: Prediction of Potential Hazardous Effects of Chemicals in Lactuca Sativa Seed Germination. *Nereis*, **2019**, *11*, 15–30.

[15] Sánchez-Morales, M.; Sabater, F.; Muñoz, I. Effects of Urban Wastewater on Hyporheic Habitat and Invertebrates in Mediterranean Streams. *Science of the Total Environment*, **2018**, *642*, 937–945. https://doi.org/10.1016/j.scitotenv.2018.06.132.

[16] Ziajahromi, S.; Neale, P. A.; Leusch, F. D. L. Wastewater Treatment Plant Effluent as a Source of Microplastics: Review of the Fate, Chemical Interactions and Potential Risks to Aquatic Organisms. *Water Science and Technology*, **2016**, *74* (10), 2253–2269. https://doi.org/10.2166/wst.2016.414.

[17] Castillo-Garit, J. A.; Marrero-Ponce, Y.; Escobar, J.; Torrens, F.; Rotondo, R. A Novel Approach to Predict Aquatic Toxicity from Molecular Structure. *Chemosphere*, **2008**, *73* (3), 415–427. https://doi.org/10.1016/j.chemosphere.2008.05.024.

[18] Benigni, R.; Fan, A.; Woo, Y.; Doull, J. Carcinogenicity of the Aromatic Amines: From Structure-Activity Relationships to Mechanisms of Action and Risk a ...

[19] Kharchevnikova, N. V.; Fjodorova, N.; Vracko, M. Quantum Chemical Simulation of Cytochrome P450 Catalyzed Oxidation and Carcinogenic Potency of Benzene Derivatives Quantum Chemical Simulation of Cytochrome P450

Catalyzed Oxidation and Carcinogenic Potency of Benzene Derivatives. **2008**, No. December 2015. https://doi.org/10.1007/978-3-540-69367-3-164.

[20] Dureja, H.; Madan, A. K. Validation of Topochemical Models for the Prediction of Permeability through the Blood-Brain Barrier. *Acta Pharmaceutica*, **2007**, *57* (4), 451–467. https://doi.org/10.2478/v10007-007-0036-2.

[21] Snyder, R.; Witz, G.; Goldstein, B. D. The Toxicology of Benzene. *Environ Health Perspect*, **1993**, *100*, 293–306. https://doi.org/10.1289/ehp.93100293.

[22] Suzuki, S.; Segawa, Y.; Itami, K.; Yamaguchi, J. Synthesis and Characterization of Hexaarylbenzenes with Five or Six Different Substituents Enabled by Programmed Synthesis. *Nature Chemistry 2015 7:3*, **2015**, *7* (3), 227–233. https://doi.org/10.1038/nchem.2174.

[23] Liang, B.; He, X.; Hou, J.; Li, L.; Tang, Z. Membrane Separation in Organic Liquid: Technologies, Achievements, and Opportunities. *Advanced Materials*, **2019**, *31* (45). https://doi.org/10.1002/adma.201806090.

[24] Yoosefian, M.; Raissi, H.; Davamdar, E.; Esmaeili, A. A.; Azaroon, M. Synthesis and Theoretical Study of Intramolecular Hydrogen Bond at Two Possible Positions in Pyrazolo[1,2-b] Phthalazine. *Chin J Chem*, **2012**, *30 (4),* 779–784. https://doi.org/10.1002/cjoc.201100036.

[25] Raissi, H.; Yoosefian, M.; Mollania, F. Hydrogen Bond Studies in Substituted Imino-Acetaldehyde Oxime. *Comput Theor Chem*, **2012**, *996*, 68–75. https://doi.org/10.1016/j.comptc.2012.07.017

[26] Frisch, M. J.; Trucks, G. W.; Schlegel, H. B.; Scuseria, G. E.; Robb, M. A.; Cheeseman, J. R.; Scalmani, G.; Barone, V.; Mennucci, B.; Petersson, G. A. Gaussian 09, Revision D. 01. Gaussian, Inc., Wallingford CT 2009.

[27] Allouche, A. Gabedit—A Graphical User Interface for Computational Chemistry Software. *J Comput Chem*, **2011**, *32* (1), 174–182.

[28] Geerlings, P.; De Proft, F.; Langenaeker, W. Conceptual Density Functional Theory. *Chem Rev*, **2003**, *103* (5), 1793–1874.

[29] Yanai, T.; Tew, D. P.; Handy, N. C. A New Hybrid Exchange–Correlation Functional Using the Coulomb-Attenuating Method (CAM-B3LYP). *Chem Phys Lett*, **2004**, *393* (1–3), 51–57.

[30] Rassolov, V. A.; Pople, J. A.; Ratner, M. A.; Windus, T. L. 6-31G* Basis Set for Atoms K through Zn. *J Chem Phys*, **1998**, *109* (4), 1223–1229.

[31] Uzzaman, M.; Hasan, M. K.; Mahmud, S.; Fatema, K.; Matin, M. M. Structure-Based Design of New Diclofenac: Physicochemical, Spectral, Molecular Docking, Dynamics Simulation, and ADMET Studies. *Inform Med Unlocked*, **2021**, 100677.

[32] Petersilka, M.; Gossmann, U. J.; Gross, E. K. U. Excitation Energies from Time-Dependent Density-Functional Theory. *Phys Rev Lett*, **1996**, *76* (8), 1212.

[33] Islam, N.; Islam, M. D.; Rahman, M. R.; Matin, M. M. Octyl 6-o-Hexanoyl-β-d-Glucopyranosides: Synthesis, Pass, Antibacterial, in Silico Admet, and Dft Studies. *Current Chemistry Letters*, **2021**, *10* (4), 413–426. https://doi.org/10.5267/j.ccl.2021.5.003.

[34] Cheng, F.; Li, W.; Zhou, Y.; Shen, J.; Wu, Z.; Liu, G.; Lee, P. W.; Tang, Y. AdmetSAR: A Comprehensive Source and Free Tool for Assessment of Chemical ADMET Properties. *J Chem Inf Model*, **2012**, *52* (11), 3099–3105. https://doi.org/10.1021/ci300367a.

[35] Uddin, M. N.; Siddique, Z. A.; Mase, N.; Uzzaman, M.; Shumi, W. Oxotitanium(IV) Complexes of Some Bis-Unsymmetric Schiff Bases: Synthesis, Structural Elucidation and Biomedical Applications. *Appl Organomet Chem*, **2019**, *33* (6). https://doi.org/10.1002/aoc.4876.

[36] Uddin, M. N.; Uzzaman, M.; Das, S.; Al-Amin, Md.; Haque Mijan, Md. N. Stress Degradation, Structural Optimization, Molecular Docking, ADMET Analysis of Tiemonium Methylsulphate and Its Degradation Products. *Journal of Taibah University for Science*, **2020**, *14* (1), 1134–1146. https://doi.org/10.1080/16583655.2020.1805186.

[37] Uzzaman, M.; Hasan, M. K.; Mahmud, S.; Yousuf, A.; Islam, S.; Uddin, M. N.; Barua, A. Physicochemical, Spectral, Molecular Docking and ADMET Studies of Bisphenol Analogues; A Computational Approach. *Inform Med Unlocked*, **2021**, *25*, 100706. https://doi.org/10.1016/j.imu.2021.100706.

[38] Kabir, E.; Noyon, M. R. O. K.; Amjad Hossain, Md.; Acharjee, P. DFT and Pharmacokinetic Study of Some Heterocyclic Aspirin Derivatives as The Cyclooxygenase Inhibitors: An In-Silico Approach. *Pharmacognosy Journal*, **2023**, *14* (6s), 1005–1021. https://doi.org/10.5530/pj.2022.14.204.

[39] Lewis, D. F. V.; Ioannides, C.; Parke, D. V. Interaction of a Series of Nitriles with the Alcohol-Inducible Isoform of P450: Computer Analysis of Structure-Activity Relationships. *Xenobiotica*, **1994**, *24* (5), 401–408. https://doi.org/10.3109/00498259409043243.

[40] Saravanan, S.; Balachandran, V. Quantum Chemical Studies, Natural Bond Orbital Analysis and Thermodynamic Function of 2,5-

Dichlorophenylisocyanate. *Spectrochim Acta A Mol Biomol Spectrosc*, **2014**, *120*, 351–364. https://doi.org/10.1016/j.saa.2013.10.042.

[41] Aihara, J. Reduced HOMO - LUMO Gap as an Index of Kinetic Stability for Polycyclic Aromatic Hydrocarbons. **1999**, 7487–7495.

[42] Scrocco, E.; Tomasi, J. The Electrostatic Molecular Potential as a Tool for the Interpretation of Molecular Properties. *New Concepts II*, **2007**, 95–170. https://doi.org/10.1007/3-540-06399-4_6.

[43] Politzer, P.; Murray, J. S. Molecular Electrostatic Potentials. *ChemInform*, **2004**, *35* (27). https://doi.org/10.1002/chin.200427290.

[44] Ramalingam, S.; Karabacak, M.; Periandy, S.; Puviarasan, N.; Tanuja, D. Spectroscopic (Infrared, Raman, UV and NMR) Analysis, Gaussian Hybrid Computational Investigation (MEP Maps/HOMO and LUMO) on Cyclohexanone Oxime. *Spectrochim Acta A Mol Biomol Spectrosc*, **2012**, *96*, 207–220. https://doi.org/10.1016/j.saa.2012.03.090.

[45] Berthomieu, C.; Hienerwadel, R. Fourier Transform Infrared (FTIR) Spectroscopy. *Photosynth Res*, **2009**, *101* (2–3), 157–170. https://doi.org/10.1007/s11120-009-9439-x.

[46] Green, J. H. S.; Harrison, D. J.; Kynaston, W. Vibrational Spectra of Benzene Derivatives—XV. *Spectrochim Acta A*, **1972**, *28* (1), 33–44. https://doi.org/10.1016/0584-8539(72)80007-2.

[47] Coates, J. Interpretation of Infrared Spectra, A Practical Approach. *Encyclopedia of Analytical Chemistry*, **2006**, 10815–10837. https://doi.org/10.1002/9780470027318.a5606.

[48] Florio, G. M.; Zwier, T. S.; Myshakin, E. M.; Jordan, K. D.; Sibert, E. L. Theoretical Modeling of the OH Stretch Infrared Spectrum of Carboxylic Acid Dimers Based on First-Principles Anharmonic Couplings. *Journal of Chemical Physics*, **2003**, *118* (4), 1735–1746. https://doi.org/10.1063/1.1530573.

[49] Tariq, M.; Ali, S.; Ahmad, F.; Ahmad, M.; Zafar, M.; Khalid, N.; Khan, M. A. Identification, FT-IR, NMR (1H and 13C) and GC/MS Studies of Fatty Acid Methyl Esters in Biodiesel from Rocket Seed Oil. *Fuel Processing Technology*, **2011**, *92* (3), 336–341. https://doi.org/10.1016/j.fuproc.2010.09.025.

[50] Subramanian, N.; Sundaraganesan, N.; Jayabharathi, J. Molecular Structure, Spectroscopic (FT-IR, FT-Raman, NMR, UV) Studies and First-Order Molecular Hyperpolarizabilities of 1,2-Bis(3-Methoxy-4-Hydroxybenzylidene) Hydrazine by Density Functional Method. *Spectrochim Acta A Mol Biomol Spectrosc*, **2010**, *76* (2), 259–269. https://doi.org/10.1016/j.saa.2010.03.033.

[51] Sallam, H. A.; Elgubbi, A. S.; El-Helw, E. A. E. Synthesis and Antioxidant Screening of New 2-Cyano-3-(1,3-Diphenyl-1H-Pyrazol-4-Yl) Acryloyl Amide Derivatives and Some Pyrazole-Based Heterocycles. *Synth Commun*, **2020**, *50* (13), 2066–2077. https://doi.org/10.1080/00397911.2020.1765258.

[52] Coates, J. Interpretation of Infrared Spectra, A Practical Approach. *Encyclopedia of Analytical Chemistry*, **2006**, 10815–10837. https://doi.org/10.1002/9780470027318.a5606.

[53] Lengauer, T.; Rarey, M. Computational Methods for Biomolecular Docking. *Curr Opin Struct Biol*, **1996**, *6* (3), 402–406. https://doi.org/10.1016/S0959-440X(96)80061-3.

[54] Wade, R. C.; Goodford, P. J. The Role of Hydrogen-Bonds in Drug Binding. *Prog Clin Biol Res*, **1989**, *289*, 433–444.

[55] Gill, D. M.; Ana, A. P.; Zazeri, G.; Shamir, S. A.; Mahmoud, A. M.; Wilkinson, F. L.; Alexander, M. Y.; L. Cornelio, M.; Jones, A. M. The Modulatory Role of Sulfated and Non-Sulfated Small Molecule Heparan Sulfate-Glycomimetics in Endothelial Dysfunction: Absolute Structural Clarification, Molecular Docking, and Simulated Dynamics, SAR Analyses and ADMET Studies. *RSC Med Chem*, **2021**, *12* (5), 779–790. https://doi.org/10.1039/d0md00366b.

[56] Shen, J.; Cheng, F.; Xu, Y.; Li, W.; Tang, Y. Estimation of ADME Properties with Substructure Pattern Recognition. *J Chem Inf Model*, **2010**, *50* (6), 1034–1041. https://doi.org/10.1021/ci100104j.

[57] Bickerton, G. R.; Paolini, G. V.; Besnard, J.; Muresan, S.; Hopkins, A. L. Quantifying the Chemical Beauty of Drugs. *Nat Chem*, **2012**, *4* (2), 90–98. https://doi.org/10.1038/nchem.1243.

[58] Veber, D. F.; Johnson, S. R.; Cheng, H. Y.; Smith, B. R.; Ward, K. W.; Kopple, K. D. Molecular Properties That Influence the Oral Bioavailability of Drug Candidates. *J Med Chem*, **2002**, *45* (12), 2615–2623. https://doi.org/10.1021/jm020017n.

[59] Amin, M. L. P-Glycoprotein Inhibition for Optimal Drug Delivery. *Drug Target Insights*, **2013**, *2013* (7), 27–34. https://doi.org/10.4137/DTI.S12519.

[60] Wilkin, M. Cost Shifting and the Quality Use of Medicines. *Aust Prescr*, **2015**, *38* (1), 4–5. https://doi.org/10.18773/austprescr.2015.007.

[61] Lamothe, S. M.; Guo, J.; Li, W.; Yang, T.; Zhang, S. The Human Ether-a-Go-Go-Related Gene (HERG) Potassium Channel Represents an Unusual Target for Protease-Mediated Damage. *Journal of Biological Chemistry*, **2016**, *291* (39), 20387–20401. https://doi.org/10.1074/jbc.M116.743138.

[62] [62] Valavanidis, P. A.; Vlachogianni, T. "Carcinogenic Chemicals: Classification and Evaluation of Carcinogenic Risk to Humans by International Organizations and the European Union." **2010**, No. April.

[63] Yost, E. E.; Stanek, J.; Dewoskin, R. S.; Burgoon, L. D. Overview of Chronic Oral Toxicity Values for Chemicals Present in Hydraulic Fracturing Fluids, Flowback, and Produced Waters. *Environ Sci Technol*, **2016**, *50* (9), 4788–4797. https://doi.org/10.1021/acs.est.5b04645.

[64] Zhu, H.; Martin, T. M.; Ye, L.; Sedykh, A.; Young, D. M.; Tropsha, A. Quantitative Structure-Activity Relationship Modeling of Rat Acute Toxicity by Oral Exposure. *Chem Res Toxicol*, **2009**, *22* (12), 1913–1921. https://doi.org/10.1021/tx900189p.

[65] Cheng, F.; Ikenaga, Y.; Zhou, Y.; Yu, Y.; Li, W.; Shen, J.; Du, Z.; Chen, L.; Xu, C.; Liu, G.; et al. In Silico Assessment of Chemical Biodegradability. *J Chem Inf Model*, **2012**, *52* (3), 655–669. https://doi.org/10.1021/ci200622d.

[66] Uzzaman, M.; Hasan, M. K.; Mahmud, S.; Fatema, K.; Matin, M. M. Structure-Based Design of New Diclofenac: Physicochemical, Spectral, Molecular Docking, Dynamics Simulation, and ADMET Studies. *Inform Med Unlocked*, **2021**, *25*, 100677. https://doi.org/10.1016/j.imu.2021.100677.

[67] Azab, A.; Nassar, A.; Azab, A. N. Anti-Inflammatory Activity of Natural Products. *Molecules*, **2016**, *21* (10), 1–19. https://doi.org/10.3390/molecules21101321.

[68] De Clercq, E. Strategies in the Design of Antiviral Drugs. *Nat Rev Drug Discov*, **2002**, *1* (1), 13–25. https://doi.org/10.1038/nrd703.

[69] J, K.; D, C.; M, R. Molecular Docking, Drug-Likeness Studies and ADMET Prediction of Quinoline Imines for Antimalarial Activity. *J Med Chem Drug Des*, **2019**, *2* (1), 1–7. https://doi.org/10.16966/2578-9589.113.